Carbon nanotube reinforced ceramics

Gan Lin Hwang and Kuo Chu Hwang*

Department of Chemistry, National Tsing Hua University, Hsinchu, Taiwan.
E-mail: kchwang@mx.nthu.edu.tw

Silicon dioxide glass rods of micrometer sizes were synthesized by using surfactant–carbon nanotube co-micelles as templates. These glass rods were used as additives to reinforce inorganic ceramics. The mechanical strength of the silicon dioxide ceramic is enhanced by $\sim100\%$ in the presence of ~6 wt% of CNTs.

Introduction

Carbon nanotubes (CNTs) were discovered by Iijima in 1991.[1] Since then, many efforts have been devoted to studying the physical properties of this new form of seamlessly perfect carbon allotrope.[2–5] In the literature, it is known that CNTs are elastic and stiff.[2–5] The Young's modulus of a CNT is of the order of ~1000 GPa.[3] Therefore, it is generally expected that CNTs can be used as additives to reinforce strengths of composite materials, such as epoxy,[6] petroleum pitch,[7] PMMA,[8] and alumina composites.[9] However, addition of CNTs into epoxy was found not to enhance the strength, owing to weak interactions between CNTs and the polymer matrix.[6] When added to an alumina composite by the hot press and hot extrusion method,[9] the mechanical strength of the alumina composite is not enhanced, a fact attributed to aggregation (or inhomogeneous dispersion) of CNTs in the composite materials (owing to very strong van der Waals interactions, CNTs always form aggregates). Good dispersion of CNTs in a matrix of composite materials, especially in inorganic materials, indeed is a significant problem, but is also a prerequisite for its application as additives for reinforcement of composite materials. Previously, it was reported that nonionic surfactants were used to aid dispersion of CNTs in acetone–polymer solutions.[10] However, how surfactant molecules help dispersion of CNTs in acetone is still not clear. In this paper, we resolve the above aggregation problem by using surfactants to aid dispersion of CNTs. Surfactants and CNTs form co-micelles, which were used as templates to synthesize SiO_2–CNT microrods. Addition of these SiO_2–CNT microrods leads to reinforcement of inorganic ceramics.

Experimental

CNTs were prepared by creating an electric arc between two graphite electrodes under 760 Torr Ar and a dc electric field (20 V, 100 A). The inner core of the cathode deposit contains 40–60% CNTs and carbon nanoparticles, which were purified by refluxing in concentrated H_2SO_4 and HNO_3 (3:2 volume ratio, 98% and 70%, respectively) for 3 h to remove the amorphous carbon.[11] The purified CNTs were then used to prepare SiO_2–CNT microrods. In a typical experiment, 6 mg of CNTs were added to 40 ml, 1.2 mM cetyltrimethylammonium bromide (C_{16}TMAB, 99+%, ACROS) aqueous solution, followed by ultrasonication to disperse the CNTs. To the CNT–surfactant solution was added 0.2 g sodium silicate (27% SiO_2 and 8% Na_2O, Merck), and 2 mg sodium aluminate (54%, AJAX Chemicals), and sonication was performed for 10 min. The solution was then slowly titrated (drop by drop) by ~6 ml of a 46 mM H_2SO_4 solution to adjust the pH to ~9.5, which

initiates polymerizaton of silicates.[12] After an additional 20 min of stirring, the final solution was put into an autoclave and heated at $\sim110\,^{\circ}C$ for 48 h. Prolonged heating inside an autoclave leads to further polymerization of silicates and formation of yellowish silicate powders. The silicate powders were washed with distilled water several times, then calcined in air at $400\,^{\circ}C$ to oxidatively remove surfactant molecules. Under a scanning electron microscope (SEM), the final silicate powder consists of long rod shape particles of micrometer lengths. Various wt% of these micrometer sized SiO_2–CNT rods were mixed with SiO_2 powder and pressed into a disc under a high pressure of $1000\,kg\,cm^{-2}$. The composite disc was then calcined in air at $400\,^{\circ}C$ for 5 h, followed by calcination in N_2 atmosphere at $1050\,^{\circ}C$ for 40 h. The hardness of the final composite discs was measured using a Vicker's hardness tester (Model MV-1, Matsuzawa Seiki Co., Ltd.) at a load of 1 kg.

In the fluorescence experiments, various amounts (0, 0.9, 1.8, or 4.2 mg) of CNTs were added into 100 ml, 1 μM 1-pyrenecarboxylic acid (Aldrich, 98%) aqueous solution, and the solution was sonicated to disperse the CNTs. Different amounts of C_{16}TMAB were then added to the solution, followed by sonication. The fluorescence intensities (Jasco, model FP-777, $\lambda_{ex} = 345$ nm) of 1-pyrenecarboxylic acid at 390 and 505 nm were measured as a function of the C_{16}TMAB concentration.

Results and discussion

In order to avoid formation of aggregates, CNTs were mixed with C_{16}TMAB surfactant in aqueous solution. Before the addition of surfactants, CNTs exist as a suspension in and eventually precipitate at the bottom of an aqueous solution. In the presence of surfactants, CNTs form co-micelle structures with surfactant molecules (*vide infra*) *via* strong van der Waals interactions and can be well dispersed in the aqueous solution, which is evident from the homogeneous black color of the solution. These cationic surfactant–CNT co-micelles were used as templates for the synthesis of silicon dioxide glass rods by addition of sodium silicate to the CNT–surfactant aqueous solution. Due to electrostatic interactions, silicate anions will adsorb onto the surface of the cationic surfactant–CNT co-micelles. Upon lowering the pH of the solution slowly from 11 to 9.5, cross-linking (or polymerization) of silicates occurs. The solution was then put in a hydrothermal reactor to accelerate polymerization of silicates. The polymerization process of silicates was the same as that used for production of MCM-41 zeolites.[13] The concentration of C_{16}TMAB surfactant used in this study is slightly above its critical micelle concentration (cmc)[14] of 0.8 mM, and liquid crystal micelle nanorods do not form. In typical procedures in the synthesis of MCM-41

Fig. 1 Scanning electron microscopy (Hitachi, model S-2300) image of SiO_2–CNT glass rods.

zeolites, very high surfactant concentrations are always used where long liquid crystal surfactant rods form and are used as templates for the synthesis of MCM-41 zeolites. The final products of the silicate–surfactant–CNT solution were examined by scanning electron microscopy (SEM). As shown in Fig. 1, sodium silicates processed by the above procedure form micrometer size glass rods. These glass rods have lengths in the range of 10–50 μm, and diameters 0.5–1.5 μm. The yield of glass rods is about 80%. Besides the glass rods, some irregular SiO_2 particles are also present.

In order to prove that CNTs and surfactant molecules indeed form co-micelle structures, a fluorescence probe, 1-pyrenecarboxylic acid, was added to monitor the formation of CNT–surfactant self-assembled co-micelle structures. Photo-excited 1-pyrenecarboxylic acid emits fluorescence at 390 and 410 nm (see Fig. 2(a)). Excited pyrene can also form an excimer with

Fig. 2 (a) Fluorescence spectra of 1 μM 1-pyrenecarboxylic acid in water in the presence of 0.8 mM (upper trace at 500 nm) and 0.2 mM (lower trace at 500 nm) of C_{16}TMAB. The excitation wavelength is 345 nm. (b) The fluorescence intensity ratio of the excimer band (505 nm) to the monomer band (390 nm), I_{ex}/I_{mo}, as a function of the surfactant concentration in the absence (●) and presence of CNTs, 0.9 mg ml^{-1} (■), 1.8 mg ml^{-1} (▲) and 4.2 mg ml^{-1} (▼).

another ground state pyrene molecule. As shown by the filled circles of Fig. 2(b), micelles are formed when the concentration of surfactant is higher than its cmc (critical micelle concentration) value of 0.8 mM. The presence of micelles leads to the formation of a broad pyrene excimer band at ~505 nm. The intensity of the excimer band is proportional to the local concentration of pyrene. The ratio of excimer *vs.* monomer (I_{ex}/I_{mo}) bands increases at higher pyrene concentrations. At a given constant pyrene concentration, the I_{ex}/I_{mo} ratio may fluctuate according to the variation of the local pyrene concentrations in a heterogeneous system, and thus can serve as a probe to monitor the change in the volume of a non-polar domain. In the current system, the I_{ex}/I_{mo} ratio was measured as a function of the surfactant concentration in the presence of various amounts of CNTs in the aqueous solution. As shown in Fig. 2(b), in the absence of CNTs (filled circles), the I_{ex}/I_{mo} ratio increases monotonically to reach a maximum at the cmc (0.8 mM), then decreases at higher C_{16}TMAB concentrations. Below the cmc, the non-polar tails of surfactant molecules probably form aggregates with the non-polar pyrene moieties, and promote the formation of excimers. At and above the cmc, micelles are formed, and the interior space of the micelles provides a non-polar environment for non-polar pyrene molecules to gather together. Therefore excimer formation is significantly enhanced as the surfactant concentration approaches the cmc value. Further increasing the C_{16}TMAB concentration above the cmc increases the micelle concentration and therefore the non-polar volume, which leads to dilution of local pyrene concentrations within each micelle. Consequently, the formation of excimers decreases continuously at high C_{16}TMAB concentrations. In the presence of CNTs (see filled squares and triangles in Fig. 2(b)), two features are noticed: (i) the onset formation of excimers occurs at lower C_{16}TMAB concentrations as compared with pure surfactant alone, and (ii) the maximum I_{ex}/I_{mo} ratio becomes smaller for higher CNT concentrations. The earlier onset formation of excimers suggests that CNTs and surfactants form hemi- or co-micelle structures and provide non-polar domains for pyrene moieties to gather together and form excimers. The smaller I_{ex}/I_{mo} ratio around the cmc region is also consistent with the formation of surfactant–CNT co-micelles. At a given surfactant concentration, a larger amount of CNTs forms more co-micelles (with surfactant molecules) and provides a higher non-polar volume than surfactant alone, which leads to lower local pyrene concentrations in the non-polar domain and thus lower probabilities of excimer formation.

With surfactant–CNT co-micelles as templates, sodium silicates form micrometer size glass rods while in the absence of CNTs, silicates do not have a well defined shape or form. To examine their internal structure, the silicon dioxide glass rods were embedded in epoxy resin, and cut with a diamond blade into thin slices. As shown in Fig. 3(a), scanning electron microscopy (SEM) shows that the internal structures of these silicon dioxide glass rods contain many irregular holes. These holes are probably formed due to copolymerization of silicate–surfactant–CNT co-micelles with silicate–surfactant–carbon nanoparticles (or amorphous carbons). Similar to CNTs, amorphous carbons and nanoparticles can also form co-micelles with surfactant molecules, and can also serve as templates for the self-assembly of silicates. During silicate polymerization processes, all surfactant–CNT (or amorphous carbons) co-micelles tend to self assemble together and form long rods. To search for evidence for the presence of CNTs within glass rods, the silicon dioxide glass rods were hand ground in a marble disc and then examined under a transmission electron microscope (TEM). As shown in Fig. 3(b), some CNTs sticking out of the end of a glass rod can be observed and are roughly parallel to each other. The fact that a glass rod contains many CNTs indicates that silicate–surfactant–CNT co-micelles have a tendency to align in parallel
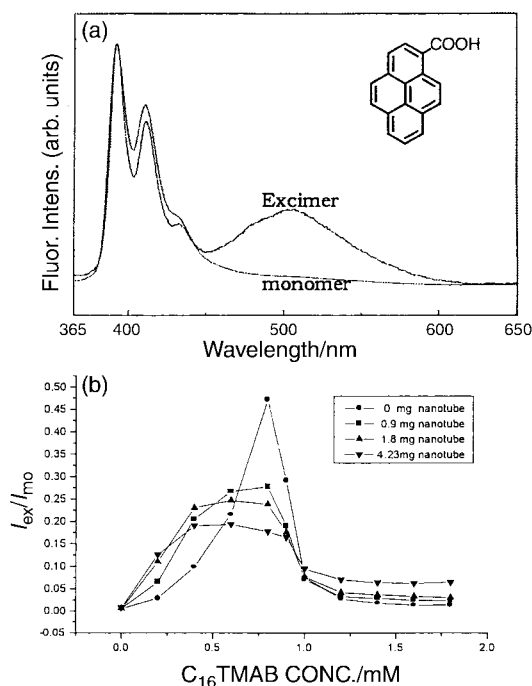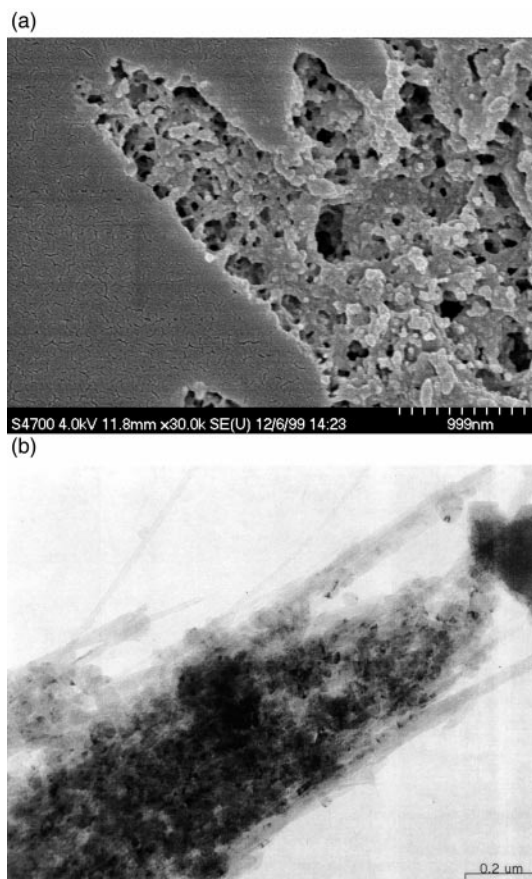
(a)

(b)

Fig. 3 (a) An SEM image of SiO2–CNT glass rods embedded in epoxy resin. (b) A TEM image (JEOL, TEM 2010, 200 kV) of the end of a SiO2–CNT glass rod.

and so form large diameter glass rods. The formation mechanism of glass rods might be postulated as similar as the silicate rod assembly mechanism of MCM-41.[15] The silicate (which is negatively charged at the high pH values used) preferentially interacts with the positively charged ammonium head groups of the surfactants and condenses into a solid. Under the synthesis conditions, the formation of glass rods begins with the deposition of two to three monolayers of silicate precursor onto isolated surfactant–CNT co-micelle rods. These silicate-encapsulated rods are initially randomly ordered (with some silicate-encapsulated particles), but eventually pack into a micro-rod structure. Heating and aging then completes the condensation of the silicates into the as-synthesized glass micro-rod structures.

By forming micrometer size glass rods, CNTs can be dispersed. These glass microrods were then mixed with SiO2 powders, and pressed into tablet discs. The composite discs were then calcined in air to oxidatively remove all surfactant molecules. Then, these glass discs were further calcined in N2 at 1323 K for 40 h to further solidify the structure. The final glass discs were examined for hardness. As shown in Fig. 4, the Vicker's hardness was plotted as a function of the wt% of CNT-containing glass rods. The hardness of composite discs increases proportionally to the percentage of the SiO2–CNT glass rods. The hardness of composite discs containing 60 wt% SiO2–CNT glass rods increases by ~100%, as compared to a pure SiO2 disc. It should be noted that the weight percentage of CNTs in the composite disc is only ~6 wt%. The evidence in Fig. 4 indicated that glass rods indeed led to the reinforcement of ceramics. To further examine whether CNTs or the outer SiO2 coating (or both) contributes to the increase in the strength, SiO2 micro-rods without CNTs were synthesized according to the literature procedure.[13b,c] As shown in Fig. 4,
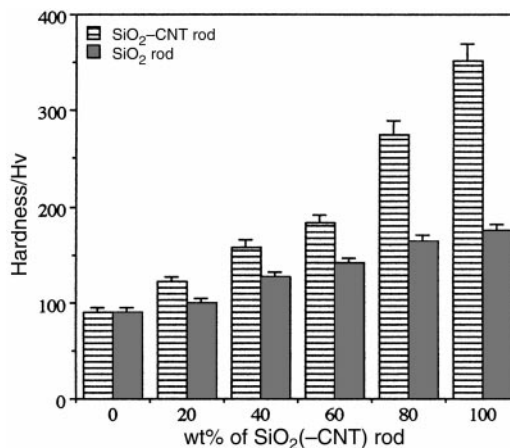

Fig. 4 The Vicker's hardness as a function of the wt% of the SiO2–CNT and SiO2 glass rods. The error bar is ±8%.

addition of micrometer sized SiO2 rods without CNTs also results in an increase of the hardness of ceramics. The increases in hardness, however, are less than those of SiO2–CNT glass rods. The results in Fig. 4 clearly indicate that both the SiO2 outer coating and CNTs contribute to an increase in the hardness of inorganic ceramics.

In order to elucidate how SiO2–CNT glass rods increase the hardness of inorganic ceramics, the fracture surfaces of the above composite discs were examined by SEM after the Vicker's hardness measurements. As shown in Fig. 5(a), the pyramidal diamond head of the Vicker's hardness meter causes a rhombus shape hole. Looking at the edge of the indentation
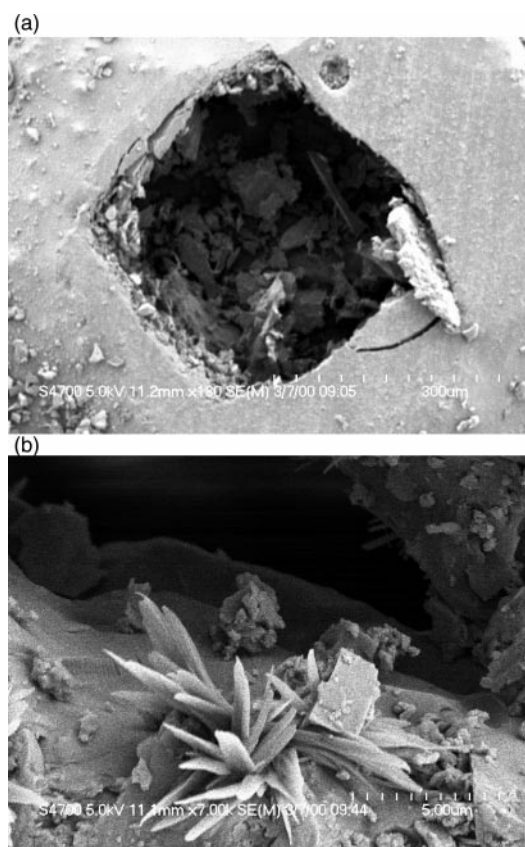

(a)

(b)

Fig. 5 SEM images of a fractured SiO2 composite disc after the Vicker's hardness measurements. (a) A rhombus shape hole created by the impact of the pyramidal shaped diamond head of a Vicker's hardness meter. (b) View of the side wall inside the rhombus hole in (a).

mark, it is observed that some SiO$_2$–CNT glass rods remain intact and stick out of the side wall (see Fig. 5(b)). It seems that the surfaces near the edge of the indentation mark were bored under tension and the bending stress led to the pulling out of the glass rods. The result in Fig. 5(b) shows that the mechanical strength of SiO$_2$–CNT glass rods is stronger than the interface strength between the glass rod and the matrix; and fracture occurs at the glass rod–matrix interface. To increase the hardness of ceramics, the added fibers have to bridge between two sides of cracks. At higher percentages of added fibers, the higher the probability that cracks will encounter the added fibers, and therefore the higher the hardness.

When a 1 kg load was used in the hardness measurements, the indentation marks were very clear-cut with sharp edges in all samples. In order to see the fracture surface and to obtain more information about the breakage of the SiO$_2$–CNT composite ceramic, a 5 kg load was used under the condition of Fig. 5(a). In Fig. 5(a), the surface near the edge of indentation mark was bored with tension and the bending stress caused edge fracture and the glass rods were pulled out. If the mechanical strength of the SiO$_2$–CNT glass rods is weaker than the interactions between the glass rod and the matrix, these glass rods will be broken instead of detaching from the matrix. The SEM image in Fig. 5(b) shows that many SiO$_2$–CNT glass rods are still intact. Therefore, it can be deduced that the mechanical strength of the SiO$_2$–CNT glass rods is stronger than the interactions between the glass rods and the matrix.

In summary, we have shown that due to strong non-polar interactions, CNTs and surfactants readily form co-micelle structures, which can be used as templates to synthesize SiO$_2$–CNT glass rods of micrometer sizes. This template synthesis method provides an easy route to well dispersed CNTs. With the inorganic SiO$_2$ outer coating, CNTs will be well mixed in inorganic materials, and provide reinforcement effects. In the presence of ~6 wt% CNTs, the hardness of SiO$_2$ composite discs can be enhanced by ~100%. Our results represent the first example where CNTs can be successfully used as reinforcement fibers to enhance the hardness of inorganic ceramics. Besides SiO$_2$ composite discs, we believe that the current SiO$_2$–CNT glass rods can also be used to reinforce other inorganic ceramic composite materials.

References

1   S. Iijima, *Nature*, 1991, **354**, 56.
2   (*a*) J. F. Despres, E. Daguerre and K. Lafdi, *Carbon*, 1995, **33**, 87; (*b*) P. Poncharal, Z. L. Wang, D. Ugarte and W. A. de Heer, *Science*, 1999, **283**, 1513.
3   (*a*) R. S. Ruoff, J. Tersoff, D. C. Lorents, S. Subramoney and B. Chan, *Nature*, 1993, **364**, 514; (*b*) J. P. Salvetat, J.-M. Bonard, N. H. Thomson, A. J. Kulik, L. Forro, W. Benoit and L. Zuppiroli, *Appl. Phys. A*, 1999, **69**, 255; (*c*) M. F. Yu, O. Lourie, M. J. Dyer, K. Moloni, T. F. Kelly and R. S. Ruoff, *Science*, 2000, **287**, 637.
4   M. M. Treacy, T. W. Ebbesen and J. M. Gibson, *Nature*, 1996, **381**, 678.
5   M. F. Yu, O. Lourie, M. J. Dyer, K. Moloni, T. F. Kelly and R. S. Ruoff, *Science*, 2000, **287**, 637.
6   L. S. Schadler, S. C. Giannaris and P. M. Ajayan, *Appl. Phys. Lett.*, 1998, **73**, 3842.
7   R. Andrews, D. Jacques, A. M. Rao, T. Rantell, F. Derbyshire, Y. Chen, J. Chen and R. C. Haddon, *Appl. Phys. Lett.*, 1999, **75**, 1329.
8   Z. Jia, Z. Wang, C. Xu, J. Liang, B. Wei, D. Wu and S. Zhu, *Mater. Sci. Eng.*, 1999, **A271**, 395.
9   T. Kuzumaki, K. Miyazawa, H. Ichinose and K. Ito, *J. Mater. Res.*, 1998, **13**, 2445.
10 I. C. Kao, Y. L. Hwang, C. P. Cheng, W. J. Wang, B. C. Wang and K. C. Hwang, *Fullerene Sci. Tech.* 2001, **9**, in press.
11 (*a*) F. Miyaji, S. A. Davis, J. P. H. Charmant and S. Mann, *Chem. Mater.*, 1999, **11**, 3021; (*b*) W. Shenton, T. Douglas, M. Young, G. Stubbs and S. Mann, *Adv. Mater.*, 1999, **11**, 253.
12 X. Gong, J. Liu, S. Baskaran, R. D. Voise and J. S. Young, *Chem. Mater.*, 2000, **12**, 1049.
13 (*a*) J. S. Beck, J. C. Vartuli, W. J. Roth, M. E. Leonowicz, C. T. Kresge, K. D. Schmitt, C. T.-W. Chu, D. H. Olson, E. W. Sheppard, S. B. McCullen, J. B. Higgins and J. L. Schlenker, *J. Am. Chem. Soc.*, 1992, **114**, 10834; (*b*) H. P. Lin and C. Y. Mou, *Science*, 1996, **273**, 765; (*c*) H. P. Lin, C. Y. Mou and S. B. Liu, *Adv. Mater.*, 2000, **12**, 103.
14 K. P. Ananthapadmanabhan, E. D. Goddard, N. J. Turro and P. L. Kuo, *Langmuir*, 1985, **1**, 352.
15 C.-Y. Chen, S. L. Burkett, H.-X. Li and M. E. Davies, *Microporous Mater.*, 1993, **2**, 27.